

*Proceeding Paper*

# Development of Rare Earth Elements Separation Processes from Coal Fly Ash <sup>†</sup>

**Aggelos Tsachouridis \*<sup>ID</sup>, Francis Pavloudakis and Nikolas Kiratzis \*<sup>ID</sup>**

Department of Mineral Resources Engineering, University of Western Macedonia, 50100 Kozani, Greece;  
 f.pavloudakis@gmail.com

\* Correspondence: agtsax@yahoo.gr (A.T.); nkiratzis@uowm.gr (N.K.)

† Presented at the International Conference on Raw Materials and Circular Economy, Athens, Greece,  
 5–9 September 2021.

**Abstract:** Rare Earth Elements and Yttrium (REY) constitute an important family of metals, with a wide range of applications and a massive impact on global industry. Studies have verified that the REY exist at significant concentrations in coal fly (CFA) and bottom ash (CBA). In the present contribution, the feasibility of CFA and CBA from the thermal power plant of PPC Meliti, Florina as a possible REY source is examined. Results are presented on the chemical and mineralogical analysis of the samples along with characterization of the initial material. Size separation results are also presented, as the first step in a subsequent beneficiation process for potential REY recovery.

**Keywords:** Rare Earths; Yttrium; fly ash; beneficiation; size separation



**Citation:** Tsachouridis, A.; Pavloudakis, F.; Kiratzis, N. Development of Rare Earth Elements Separation Processes from Coal Fly Ash. *Mater. Proc.* **2021**, *5*, 69. <https://doi.org/10.3390/materproc2021005069>

Academic Editor: Anthimos Xenidis

Published: 9 December 2021

**Publisher's Note:** MDPI stays neutral with regard to jurisdictional claims in published maps and institutional affiliations.



**Copyright:** © 2021 by the authors. Licensee MDPI, Basel, Switzerland. This article is an open access article distributed under the terms and conditions of the Creative Commons Attribution (CC BY) license (<https://creativecommons.org/licenses/by/4.0/>).

## 1. Introduction

Rare Earth Elements are essential raw materials for a wide variety of industrial products—from electric and hybrid vehicles to tablets and next generation mobile phones and from photovoltaic panels and wind turbines to space technology and weapon systems. Reliable and unhindered access to certain raw materials is a growing concern within the EU and across the globe. In order to address this challenge, in 2011, the EU Commission created the first CRM (Critical Raw Materials) list so as to classify these materials according to their industrial demand, their supply risk and their impact on the European Green Deal. The recent revised assessment of 2020 includes 83 individual raw materials, amongst which the REY (grouped as Heavy REY and Light REY) play a predominant role. More specifically, based on the combination of their supply risk for key technologies and their economic importance, the REY are classified as critical raw materials, having the highest supply risk amongst all 83 raw materials listed, with a relative medium economic importance [1]. The classification of the REY into Heavy and Light is based on their atomic number, with the L.REY being the elements from La to Sm (Atomic number 57 → 62) and the H.REY from Eu to Lu (Atomic Number 63 → 71) [2]. Another classification, according to Seredin and Dai [3], categorizes these elements as Critical (Nd, Eu, Tb, Dy, Y, Er), Uncritical (La, Pr, Sm, Gd) and Excessive (Ce, Ho, Tm, Yb, Lu). Based on this characterization, the above authors indicated that each potential source should ideally have a high concentration of Critical REY and a small concentration of Excessive REY (especially Ce, which is the most abundant in nature). In order to further characterize the material under investigation, the Outlook Coefficient and the Critical Percentage indexes have been introduced and described by the equations below:

$$Coutlook = \frac{(Nd + Eu + Tb + Dy + Er + Y) / \sum REY}{(Ce + Ho + Tm + Yb + Lu) / \sum REY} \quad (1)$$

$$Critical \% = \frac{(Nd + Eu + Tb + Dy + Er + Y)}{\sum REY} \times 100. \quad (2)$$

Evidently, the higher the Outlook Coefficient, the more promising the REY source with respect to its potential industrial value. According to Dai et al. [4], sources that produce an Outlook Coefficient between 0.7 and 1.9 should be considered promising. Seredin and Dai also indicated that there exist different distribution patterns of REY enrichment in different sources of coal ash. Coal ashes may be enriched in light (L-type distribution), medium (M-type), or heavy REY (H-type) in comparison with the Upper Continental Crust (UCC) which is considered as normal (N-type) [3]. These patterns indicate the geological background and the formation processes of the coal ore from which a particular type of coal ash has originated. More specifically, the L-type REY distribution pattern ( $\text{La}_\text{N}/\text{Lu}_\text{N} > 1$ ) is indicative of terrigenous or tuffaceous origin in which REY input occurred at the peat bog stage. In this type of pattern,  $C_{\text{outlook}}$  values range from 0.5 to 0.9. An M-type REY distribution pattern ( $(\text{La}_\text{N}/\text{Sm}_\text{N} < 1)$ ,  $(\text{Gd}_\text{N}/\text{Lu}_\text{N} > 1)$ ) is related to REY supply by acid hydrothermal solutions and the  $C_{\text{outlook}}$  values range from 0.8 to 1.3. Finally, the H-type REY distribution pattern ( $\text{La}_\text{N}/\text{Lu}_\text{N} < 1$ ) is related to the circulation of natural water enriched in HREY in coal basins. The  $C_{\text{outlook}}$  values range from 0.9 to 3.8 [3].

The ashes produced from the lignite combustion activity in PPC Meliti are currently utilized as materials in the environmental and surface restoration of depleted mining pits and the CFA specifically is also utilized as an admixture material in the cement industry.

Generally, it has been observed that ashes of different geological origin may respond differently to the various beneficiation methods [5]. Different combustion temperature and overall operating conditions of the different power plants also affect the beneficiation process. In the present endeavor, samples of CFA and CBA from the active thermal power plant of PPC Meliti, Florina are characterized (chemically and mineralogically) in order to assess their potential as a valuable REY source and dictate the choice of an appropriate beneficiation process. Towards this end, the effect of size separation on REY content is examined as a first step of the beneficiation process. In light of these findings, appropriate subsequent enrichment processes are proposed and discussed.

## 2. Material and Methods

### 2.1. Material

Samples of coal fly and bottom ash were collected from the active thermal power plant of PPC Meliti, Florina. A large quantity of ash was collected every day, for five days, and the material was thoroughly mixed and subjected to coning and quartering so as to produce two final samples of fly and bottom ash, representative of the material that the power plant produces on a weekly basis.

### 2.2. Analytical Methods

#### Elemental and Mineralogical Analysis

Prior to major, minor and trace element analysis, the two ash samples were subjected to thermogravimetric analysis (TGA) in an LECO TGA801 Analyzer so as to estimate the Loss on Ignition (LOI) content. LOI can be used as an approximate method to determine the quantity of the unburned carbon of any given sample. The chemical composition of the samples (major and minor elements) was examined by X-ray fluorescence (XRF) analysis. A benchtop Energy Dispersive XRF Spectrometer was utilized for the analysis [6]. The REY content of the samples was examined by Inductively Coupled Plasma—Mass Spectroscopy in the ALS Geochemistry Laboratory, Loughrea, Co. Galway, Ireland. Once the elemental composition of the two samples was fully identified, the sample with the higher REY content (CFA) was selected for further examination.

The mineralogical composition of the CFA was analyzed with X-Ray powder diffraction (XRD, Bruker 38 Advance Series II X-ray Diffractometer). The scanning parameters that were used for the analysis were a  $2\theta$  scanning interval of  $5^\circ$ – $70^\circ$ ,  $0.015^\circ/\text{step}$ , with a step time of 5 s.

### 2.3. Size Separation

Particle size separation was the first beneficiation method that was implemented and presented here so as to investigate the distribution of the REY in the different size fractions, the Enrichment Factor achieved in each size fraction and the relative (%) recovery. Size separation was carried out by means of dry sieving and for this process an ANALYSETTE 3 PRO FRITSCH Vibratory Sieve Shaker was used. The particle size ranges that were evaluated were the following: +50 Mesh ( $>297\text{ }\mu\text{m}$ ), 50–120 Mesh ( $297\text{--}125\text{ }\mu\text{m}$ ), 120–200 Mesh ( $125\text{--}75\text{ }\mu\text{m}$ ), 200–325 Mesh ( $75\text{--}44\text{ }\mu\text{m}$ ), 325–400 Mesh ( $44\text{--}37\text{ }\mu\text{m}$ ) and –400 Mesh ( $<37\text{ }\mu\text{m}$ ). For each sieving test, 80 gr of fly ash were loaded on the sieving apparatus, while each test lasted 85 min approximately. After each separation the different size fractions were weighted. The +50 Mesh and the 50–120 Mesh fractions were further pulverized so as to pass the 60 Mesh sieve, in order to be subjected to thermogravimetric analysis.

## 3. Results and Discussion

### 3.1. Material Characterization

The ICP-MS analysis revealed that the REY content of the CFA was equal to 254.7 ppm while that of the CBA was equal to 227.9 ppm, therefore the CFA sample was selected for further examination. According to the ASTM C618-12a, the CFA can be classified as Class C since the total  $\text{SiO}_2 + \text{Al}_2\text{O}_3 + \text{Fe}_2\text{O}_3$  content is within 50% and 70% while the  $\text{CaO}$  content approximates 15% [7]. In general, Class C fly ash originates from the combustion of lower-rank coals such as sub-bituminous and lignite coals. The feed material of PPC Meliti consists mainly of lignite, a fact that further confirms the type C classification for the CFA. The overall chemical composition of the two initial samples and that of the size fractions that derived from the dry sieving process is presented in Table 1. The REY distribution pattern for both fly and bottom ash samples is presented in Figure 1 (H-type).

**Table 1.** Chemical composition of the initial samples and of the various size fractions.

Elements	Bottom Ash	Fly Ash	+50 M	50–120 M	120–200 M	200–325 M	325–400 M	–400 M
$\text{SiO}_2$	38.34	41.07	31.07	31.71	38.84	39.87	40.67	41.37
$\text{Al}_2\text{O}_3$	14.86	16.89	15.12	14.56	17.09	16.93	16.85	17.08
$\text{Fe}_2\text{O}_3$	12.69	8.52	6.97	7.73	7.92	8.15	8.44	9.35
$\text{CaO}$	17.71	14.83	9.23	15.34	13.31	13.63	15.26	16.03
$\text{MgO}$	2.72	3.73	3.22	3.05	3.38	3.41	3.68	3.85
$\text{K}_2\text{O}$	1.71	2.05	1.44	1.57	1.93	1.97	2.04	2.15
$\text{Na}_2\text{O}$	1.53	2.02	0.95	1.08	0.87	1.49	1.77	2.2
$\text{SO}_3$	3.37	4.32	4.03	2.7	2.64	2.97	4.09	4.88
$\text{La}$	39.93	43.11	45.6	45.4	43.1	41.6	39.2	39.9
$\text{Ce}$	79.38	88.14	91.4	92.1	90.3	89.1	84.3	85.4
$\text{Pr}$	9.06	10.2	10.2	10.4	10.1	10.05	9.45	9.51
$\text{Nd}$	33.87	38.97	38.1	38.4	38.8	38.5	35.7	36.6
$\text{Sm}$	7.21	7.25	7.2	7.75	7.35	7.63	7.19	7.36
$\text{Eu}$	1.26	1.52	1.62	1.62	1.68	1.79	1.62	1.69
$\text{Gd}$	5.59	6.29	7.12	6.72	7.13	7.11	6.96	7.14
$\text{Tb}$	0.86	1.09	0.99	0.99	1.07	1.12	1.03	1.07
$\text{Dy}$	5.51	6.78	6.22	6.39	6.57	6.83	6.22	6.51
$\text{Ho}$	1.17	1.32	1.27	1.3	1.39	1.42	1.32	1.36
$\text{Er}$	3.45	4.02	3.8	3.82	4.08	4.22	3.92	4.11
$\text{Tm}$	0.48	0.61	0.52	0.56	0.6	0.64	0.6	0.58
$\text{Yb}$	3.29	3.82	3.86	3.76	4.22	4.07	3.84	4.15
$\text{Lu}$	0.54	0.58	0.55	0.59	0.58	0.64	0.59	0.63
$\text{Y}$	36.37	40.99	36.5	38.1	39.3	41.1	40.1	41.2
$\Sigma\text{REY}$	227.92	254.68	254.95	257.9	256.27	255.82	242.04	247.21
Critical (%)	35.67	36.66	34.22	34.63	35.71	36.57	36.61	36.89

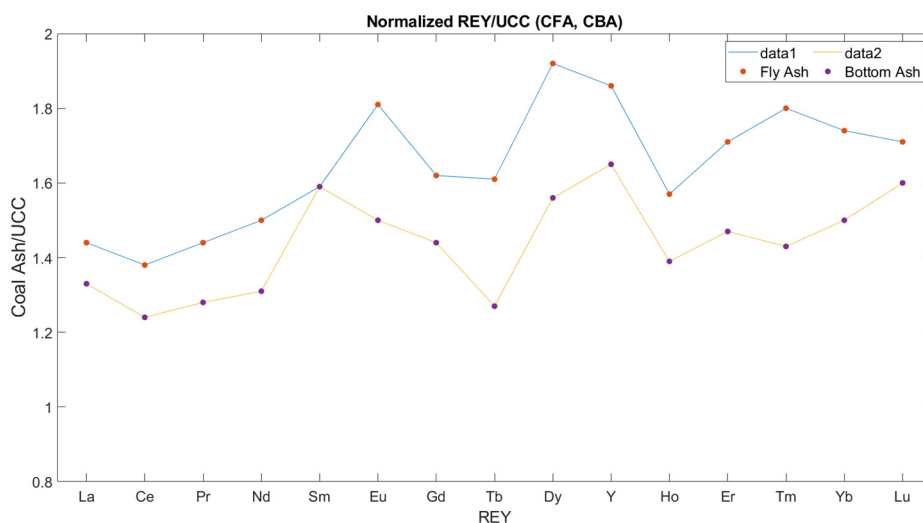


**Figure 1.** REY Distribution Pattern of the Fly and Bottom Ash Samples.

The mineral composition of the initial sample and that of all size fractions consisted of amorphous glass phase, quartz, plagioclases (albite, labradorite, bytownite), lime, gehlenite, hematite and anhydrite. The semi-quantitative XRD analysis showed that the quartz content was significantly lower in the two coarser fractions (+50 Mesh, 50–120 Mesh), increased in the 120–200 Mesh fraction and then slightly decreased towards the finer fractions. Albite was mainly observed in the coarser fractions (+50 Mesh, 50–120 Mesh) and the amorphous glass content progressively increased towards the finer particle sizes. Gehlenite and hematite content also slightly increased as the particle size decreased, while the anhydrite that was observed in the initial CFA sample was concentrated after the size separation process in the 325–400 Mesh and in the –400 Mesh sizes. A typical XRD diffractogram for the –400 Mesh fraction, which will be the focus of our discussion, is presented in Figure 2.

### 3.2. Size Separation for Potential REY Enrichment

The initial CFA sample presented a  $C_{outlook}$  value equal to 0.99 and a critical REY (%) value equal to 36.66%, as shown in Table 1. As mentioned earlier,  $C_{outlook}$  values ranging between 0.7 and 1.9 reveal a promising source, with potential industrial value. Comparatively, Blissett et al. who have investigated the REY content of Polish and United Kingdom industrial CFA's report critical REY values ranging from 33% to 35.8% and  $C_{outlook}$  between 0.84–0.96 [8]. Despite the relatively elevated values of critical REY (%) and  $C_{outlook}$  that were mentioned above, the overall REY concentration in CFA of PPC Meliti (254.7 ppm) was lower than the global average (404 ppm) [3], a fact that reinforces the necessity of implementing beneficiation methods prior to the main extraction.

As proposed by Lin et al. [9], the enrichment factor (EF) can be utilized to quantitatively characterize the REY potential enrichment that can be achieved for each size fraction while the separation efficiency can be quantified with the REY recovery (%). The enrichment factor and the REY recovery (%) are given below:

$$EF_i = \frac{REY_i}{REY_f} \quad (3)$$

$$REY \text{ recovery } (\%) = \frac{REY_i W_i}{(\sum_i^n REY_i W_i)} \times 100, \quad (4)$$

where  $REY_f$  represents the REY concentration of the feed CFA to the sieving process (expressed in ppm),  $REY_i$  represents the REY concentration of the  $i$ th size fraction (expressed in ppm),  $W_i$  represents the mass of the  $i$ th size fraction (expressed in kg),  $REY_i W_i$  represents the total mass of REY in the  $i$ th size fraction (expressed in mg),  $n$  represents the number

of the fractions that resulted from the size separation process. The results of the sieving process are presented in Figure 3 where the major elements composition and the LOI are shown at each different size fraction.

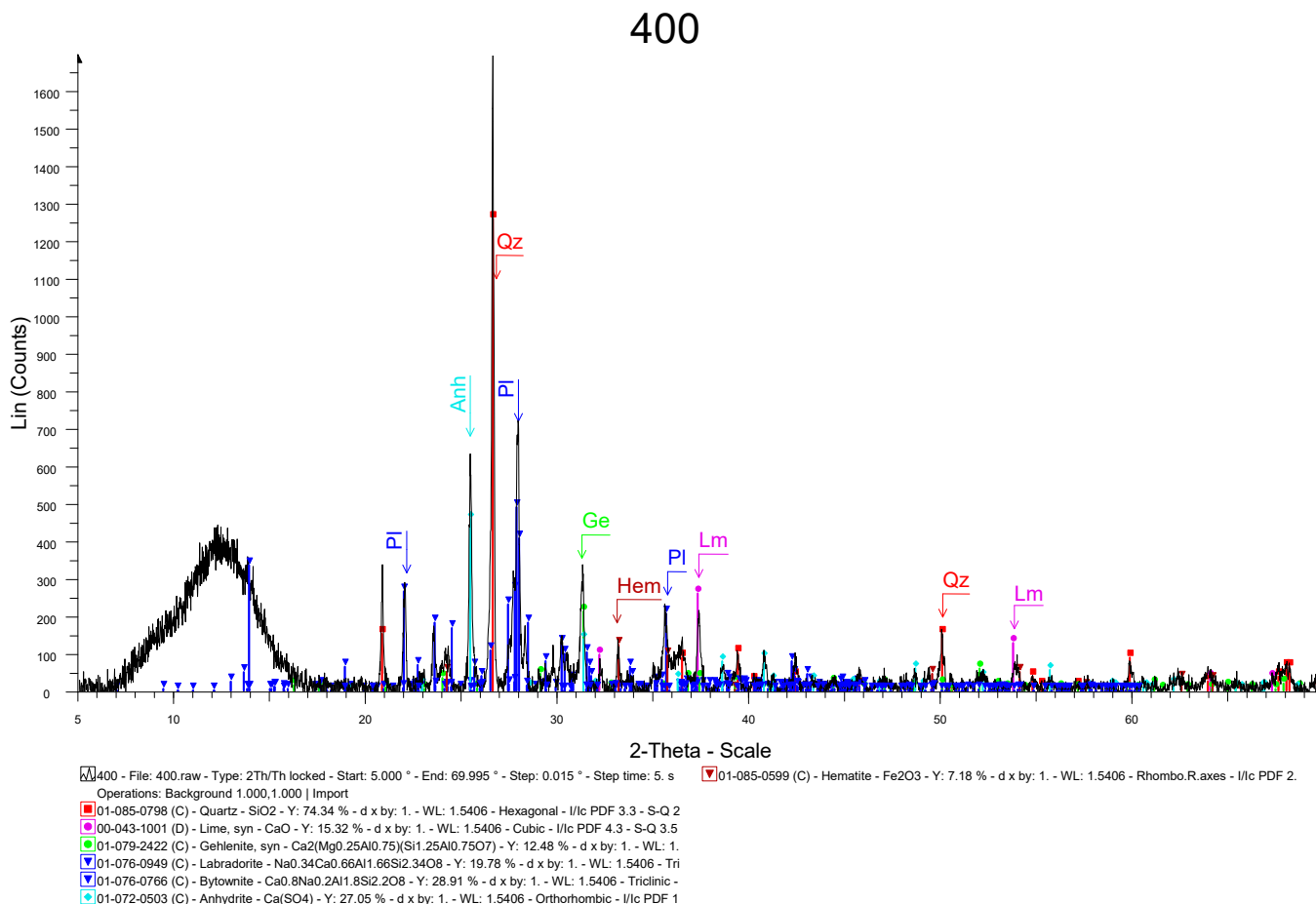


**Figure 2.** XRD Analysis for the -400 Mesh size fraction.

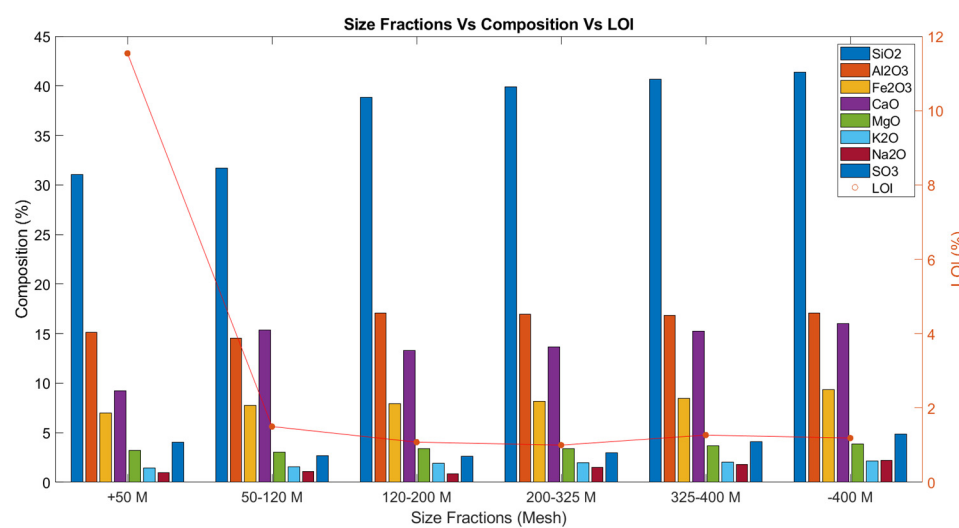


**Figure 3.** Major Elements Composition and Loss on Ignition of the different size fractions.

Figure 3 reveals that the coarser fraction (+50 Mesh) had the highest LOI content, which indicates that the majority of the unburned carbon is concentrated in that particular size fraction. It must be noted that the +50 Mesh fraction was selected under the hypothesis that the majority of the unburned carbon will be concentrated in that particle size

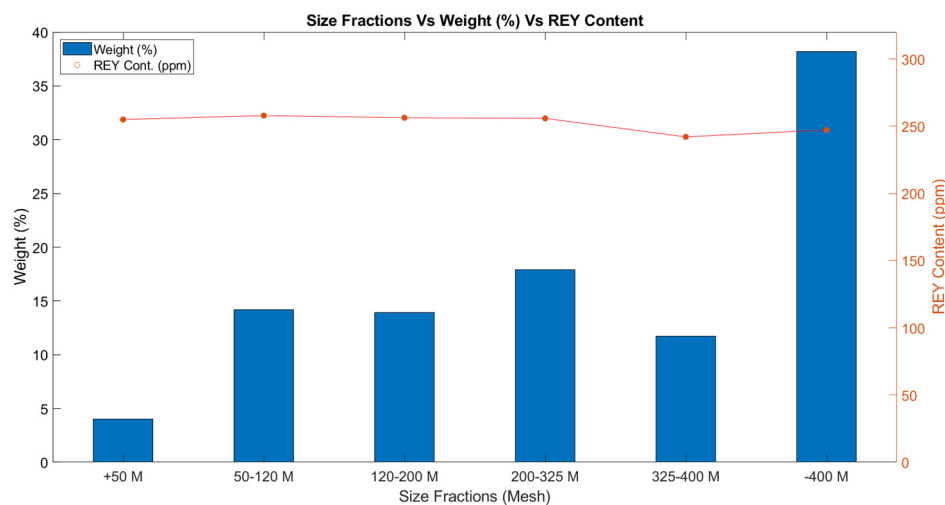
range. In general, the remaining organic material should be removed because it will inhibit a subsequent acidic-alkaline leaching extraction process that may be implemented after the physical separations. When the unburned carbon comes into contact with acids or bases, it tends to consume a portion of these lixivants and change its textural structure and functional groups [10]. Therefore, REY recovery from fly ashes containing amounts of unburned carbon, with acidic-alkaline leaching, will require higher amounts of lixivants [11]. It can be inferred that dry sieving can be used for the collection and removal of the majority of unburned carbon with the coarser fractions when more effective methods, such as froth flotation, cannot directly be implemented [8].

Table 1 shows that the  $\text{SiO}_2$  and  $\text{Fe}_2\text{O}_3$  content steadily increases with decreasing particle size. The  $\text{CaO}$  content also increases in the finer particle sizes, while those of  $\text{Al}_2\text{O}_3$  and  $\text{MgO}$  tend to remain relatively constant in all the fractions. Looking closely at both the chemical and mineralogical analysis, it can be inferred that the  $\text{SiO}_2$  concentration is more probably associated with the presence of quartz and secondarily with the amorphous glass and the presence of albite and gehlenite. On the other hand,  $\text{Al}_2\text{O}_3$  should be primarily associated with the amorphous glass phase and secondarily with the presence of albite and labradorite.  $\text{Fe}_2\text{O}_3$  content is associated with the presence of hematite in all the size fractions, while  $\text{CaO}$  is primarily associated with the presence of bytownite and secondarily with that of labradorite, gehlenite and lime. Table 2 summarizes the results of the size separation process.

**Table 2.** Size separation results.

Size Fraction	REY Conc. (ppm)	Enrichment Factor	Recovery (%)	Critical (%)
+50 Mesh	254.95	1.001	4.07	34.22
50–120 Mesh	257.9	1.013	14.59	34.63
120–200 Mesh	256.27	1.006	14.17	35.71
200–325 Mesh	255.82	1.005	18.24	36.57
325–400 Mesh	242.04	0.951	11.31	36.61
–400 Mesh	247.21	0.971	37.62	36.89

The weight percentage along with the REY content of every fraction is presented in Figure 4. It can be seen that the –400 Mesh size fraction is predominant in the PPC Meliti CFA (38.2 %), while almost 60% of the overall particles are smaller than 200 Mesh. REY content, on the other hand, does not significantly change throughout all size fractions. Figure 5 shows the effect of size separation on the REY recovery and the enrichment factor. It can be seen that recovery follows the trend of the REY content of Figure 4 as expected with approximately 38% available in the –400 Mesh fraction. Enrichment, similarly to REY content, is almost identical in all fractions. In fact, both figures indicate that size separation as a beneficiation process does not significantly affect REY content. The REY content and consequently the enrichment factor, is almost equal in all the fractions and, with its values ranging from 0.951 (in the 325–400 M fraction) to 1.013 (in the 50–120 M fraction). The fact that almost 40% of the material resides in the –400 Mesh fraction significantly increases the REY recovery (%) in that fraction to 37.62%. This actually reflects the fact that  $\text{REY recovery} (\%) = \text{EF} \times \text{Weight} (\%)$  and the EF is approximately 1, in all cases. It has already been mentioned that the  $\text{Fe}_2\text{O}_3$  content increased as the particle size decreased, a fact that indicates that the –400 Mesh size hosts a relatively larger quantity of Fe-bearing minerals. These minerals have magnetic properties and their subsequent removal, with magnetic separation, could importantly increase the REY concentration. The fact that the two finer particle sizes (325–400 M & –400 M) exhibit an enrichment factor slightly lower than 1 may also be attributed to the fact that the REY were found to exhibit negative correlation with  $\text{Fe}_2\text{O}_3$  in some previous relative studies [9,12]. Future work will involve magnetic separation, in which the magnetic fraction is expected to contain the majority of the Fe-bearing minerals so the non-magnetic fraction is expected to have higher REY content, as pointed out before. Noteworthy is also the fact that the Critical (%) increased as the particle size decreased.



**Figure 4.** REY content of the various size fractions.

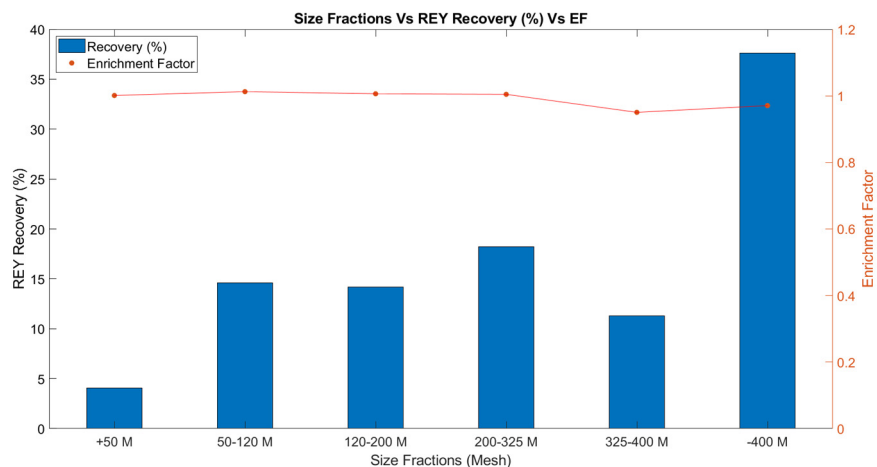


**Figure 5.** Enrichment factor and REY recovery in the various size fractions.

#### 4. Conclusions

Fly and bottom ash samples were collected from the active thermal power plant of PPC Meliti, Florina, in order to be evaluated as potential REY sources. After their chemical and mineralogical analyses and the subsequent characterization, it was confirmed that the fly ash contained higher concentrations of REY and it was selected as the basis for beneficiation. The first beneficiation method that was implemented and presented here was size separation via dry sieving. It was found that size separation did not significantly enrich REY content in a specific size fraction. Almost 40% of the material resulted in the finest fraction (~400 Mesh) a fact that led to a 37.62% recovery. The Critical (%) and the  $\text{Fe}_2\text{O}_3$  contents were also found highest in that size fraction, which indicates that subsequent magnetic separation will significantly enhance REY content, in that size range.

**Institutional Review Board Statement:** Not applicable.

**Informed Consent Statement:** Not applicable.

**Data Availability Statement:** The data presented in this study are available on request from the corresponding author.

**Acknowledgments:** This research was partially supported by the Special Research Account Committee of the University of Western Macedonia (Grant number: 70305). The authors also wish to thank Komnitsas Konstantinos and Kallithrakas Nikos (both at Technical University of Crete) for their contribution and insightful discussion.

## References

- Blengini, G.A.; Latunussa, C.E.L.; Eynard, U.; de Matos, C.T.; Wittmer, D.; Georgitzikis, K.; Pavel, C.; Carrara, S.; Mancini, L.; Unguru, M.; et al. *Study on the EU's List of Critical Raw Materials (2020) Final Report*; Publications Office of the European Union: Luxembourg, 2020. [[CrossRef](#)]
- Simoni, M.; Kuhn, E.P.; Morf, L.S.; Kuendig, R.; Adam, F. Urban mining as a contribution to the resource strategy of the Canton of Zurich. *Waste Manag.* **2015**, *45*, 10–21. [[CrossRef](#)]
- Seredin, V.V.; Dai, S. Coal deposits as potential alternative sources for lanthanides and yttrium. *Int. J. Coal. Geol.* **2012**, *94*, 67–93. [[CrossRef](#)]
- Dai, S.; Xie, P.; Jia, S.; Ward, C.R.; Hower, J.C.; Yan, X.; French, D. Enrichment of U-Re-V-Cr-Se and rare earth elements in the Late Permian coals of the Moxinpo Coalfield, Chongqing, China: Genetic implications from geochemical and mineralogical data. *Ore Geol. Rev.* **2017**, *80*, 1–17. [[CrossRef](#)]
- Rosita, W.; Bendiyasa, I.M.; Perdana, I.; Anggara, F. Sequential particle-size and magnetic separation for enrichment of rare-earth elements and yttrium in Indonesia coal fly ash. *J. Environ. Chem. Eng.* **2020**, *8*, 103575. [[CrossRef](#)]
- Hatzistavros, V.S.; Kallithrakas-Kontos, N.G. X-ray fluorescence mercury determination using cation selective membranes at sub-ppb levels. *Anal. Chim. Acta* **2014**, *809*, 25–29. [[CrossRef](#)]
- ASTM C618-12a Standard Specification for Coal Fly Ash and Raw or Calcined Natural Pozzolan for Use in Concrete. Available online: <https://www.astm.org/DATABASE.CART/HISTORICAL/C618-12A.htm> (accessed on 5 June 2021).
- Blissett, R.S.; Smalley, N.; Rowson, N.A. An investigation into six coal fly ashes from the United Kingdom and Poland to evaluate rare earth element content. *Fuel* **2014**, *119*, 236–239. [[CrossRef](#)]
- Lin, R.; Howard, B.H.; Roth, E.A.; Bank, T.L.; Granite, E.J.; Soong, Y. Enrichment of rare earth elements from coal and coal by-products by physical separations. *Fuel* **2017**, *200*, 506–520. [[CrossRef](#)]
- Wang, S.; Ma, Q.; Zhu, Z.H. Characteristics of unburned carbons and their application for humic acid removal from water. *Fuel Process. Technol.* **2009**, *90*, 375–380. [[CrossRef](#)]
- Bartoňová, L. Unburned carbon from coal combustion ash: An overview. *Fuel Process. Technol.* **2015**, *134*, 136–158. [[CrossRef](#)]
- Abedini, A.; Calagari, A.A. Rare earth element geochemistry of the Upper Permian limestone: The Kanigorreh mining district, NW Iran. *Turk. J. Earth Sci.* **2015**, *24*, 365–382. [[CrossRef](#)]